Adipose mesenchymal stem cells-derived extracellular vesicles exert their preferential action in damaged central sites of SOD1 mice rather than peripherally

Ermanna Turano,[1]* Federica Virla,[1]* Ilaria Scambi,[1] Sylwia Dabrowska,[1,2] Oluwamolakun Bankole,[3] Raffaella Mariotti[1]

[1]Department of Neurosciences, Biomedicine and Movement Sciences, University of Verona, Italy
[2]NeuroRepair Department, Mossakowski Medical Research Institute, Polish Academy of Sciences, Warsaw, Poland
[3]Department of Clinical Neurosciences, Cumming School of Medicine, University of Calgary, Alberta, Canada

*These authors contributed equally

ABSTRACT

Amyotrophic lateral sclerosis (ALS) is a neurodegenerative disorder involving motor neuron (MN) loss in the motor cortex, brainstem and spinal cord leading to progressive paralysis and death. Due to the pathogenetic complexity, there are no effective therapies available. In this context the use of mesenchymal stem cells and their vesicular counterpart is an emerging therapeutic strategy to counteract neurodegeneration. The extracellular vesicles derived from adipose stem cells (ASC-EVs) recapitulate and ameliorate the neuroprotective effect of stem cells and, thanks to their small dimensions, makes their use suitable to develop novel therapeutic approaches for neurodegenerative diseases as ALS. Here we investigate a therapeutic regimen of ASC-EVs injection in SOD1(G93A) mice, the most widely used murine model of ALS. Repeated intranasal administrations of high doses of ASC-EVs were able to ameliorate motor performance of injected SOD1(G93A) mice at the early stage of the disease and produce a significant improvement at the end-stage in the lumbar MNs rescue. Moreover, ASC-EVs preserve the structure of neuromuscular junction without counteracting the muscle atrophy. The results indicate that the intranasal ASC-EVs administration acts in central nervous system sites rather than at peripheral level in SOD1(G93A) mice. These considerations allow us to identify future applications of ASC-EVs that involve different targets simultaneously to maximize the clinical and neuropathological outcomes in ALS *in vivo* models.

Key words: amyotrophic lateral sclerosis; extracellular vesicles; stem cells; exosomes, SOD1(G93A); neuroprotection; motor neurons.

Correspondence: Raffaella Mariotti, Department of Neurosciences, Biomedicine and Movement Sciences, University of Verona, Piazzale Ludovico Antonio Scuro 10, 37134 Verona, Italy. E-mail: raffaella.mariotti@univr.it

OPEN ACCESS

Introduction

Amyotrophic lateral sclerosis (ALS) is a fatal motor neuron disease resulting in the progressive paralysis due to the degeneration of motor neurons (MNs) in the motor cortex, brainstem, and spinal cord.[1] Unfortunately, therapies are currently insufficient and only capable of slowing down the progression of the disease.[2]

Most cases are sporadic forms and only 10% of affected patients suffering from familial forms. Of these, 20% of cases are associated with mutations in the gene that codes for superoxide dismutase 1 (SOD1).[3,4] ALS mice characterized by an overexpression of mutant SOD1 are currently among the most used experimental models which reflect many similarities with the human phenotype.[5,6] This transgenic model is characterized by progressive weakness of the hind and subsequently the front limbs until death, which presumably occurs due to respiratory compromise. The animals show a progressive loss of MNs in the ventral horn of the spinal cord with inclusions of SOD1 protein and neurofilaments. Moreover, the transgenic mice display altered myofiber size with defective mitochondrial respiration, and reduced muscle functions.[7] This is accompanied by extensive astrogliosis that increases with the disease progression.[8]

Over the past twenty years, the SOD1 mouse, and primarily the SOD1(G93A) mouse model, has been used not only to characterize the pathogenesis of ALS but also to explore the effects of potential therapies.[9,10]

Among the experimental therapies, stem cell transplantation results are a promising approach to treat ALS,[11] as they have shown beneficial effects in counteracting several features of neurodegenerative process in SOD1 mice.[12]

The capabilities of stem cells to secrete bioactive molecules which simultaneously display neuroprotective and immunomodulatory properties[13,14] appear to be the mechanisms on which the rationale of stem cell therapy is based. The paracrine activity of stem cells is widely described and, in particular, among the plethora of secreted factors, those released *via* extracellular vesicles (EVs) are a promising therapeutic approach.

The regenerative and protective potential of EVs from mesenchymal stem cells (MSC-EVs) has been demonstrated in numerous *in vitro* and *in vivo* ALS models.[15-19] Thanks to their content, the EVs were able to reproduce and display therapeutic effects similar to their parental cells, avoiding possible side effects and suggesting their potential use in cell-free therapy.[20-22]

Recently, we demonstrated a neuroprotective role of EVs derived from adipose mesenchymal stem cells (ASC-EVs) administered both *via* intravenous (i.v.) and intranasal (i.n.) injections in SOD1(G93A) mice with a slowing down of disease's progression in EVs treated mice,[17] identifying and supporting the i.n. delivery as an elective route for the chronic treatment of ALS. However, no differences were observed concerning the survival of ASC-EVs treated SOD1(G93A) mice probably because, at the late phase of the disease, the applied ASC-EVs dose was inefficient.

Here we report a study to evaluate the impact of a higher dose of ASC-EVs treatment on MNs survival and neuromuscular junctions (NMJs) preservation in SOD1(G93A) transgenic mice.

Materials and Methods

ASCs culture

Murine ASCs were isolated from inguinal adipose tissues of 8-12-week-old C57Bl6/J mice (Charles River Laboratories, Sant'Angelo Lodigiano, Italy). Animals were housed in pathogen-free, climate-controlled facilities and were provided with food and water *ad libitum* according to current European Community laws. All mouse experiments were carried out in accordance with experimental guidelines approved by the University of Verona Committee on Animal Research (Centro Interdipartimentale di Servizio alla Ricerca Sperimentale, CIRSAL) and by the Italian Ministry of Health (protocol #642/2021-PR). The research complies with the commonly accepted "3Rs", minimizing the number of animals used and avoiding their suffering.

Hank's Balanced Salt Solution (HBSS, Thermo Fisher Scientifics, Carlsbad, CA, USA) with collagenase type I (Thermo Fisher Scientifics) and BSA (AppliChem, Darmstadt, Germany) were used to incubate the inguinal fat. Stromal vascular fraction (SVF) was obtained by centrifugation at 1200 g, as previously described.[23,24] Subsequently, the SVF was re-suspended in NH$_4$Cl, centrifuged at 1200 g and filtered. Murine ASCs were seeded in DMEM, 10% FBS, 100 U/mL penicillin, and 100 μg/mL streptomycin (all from GIBCO Life Technologies, Milan, Italy) and incubated at 37°C/5% CO$_2$.

The immunophenotypic analysis of murine ASCs was performed using monoclonal antibodies specific for CD106, CD9, CD44, CD80, and CD138 as well as by the absence of hematopoietic and endothelial markers (as CD45, CD11c, CD34 and CD31 respectively), as previously described.[12,23]

ASC-EVs isolation and characterization

ASC-EVs were isolated from the culture medium of murine ASCs at 14-18 passages, as previously described.[16] The cells were cultured to reach the confluence and then FBS deprived for 48 h to avoid any contamination of vesicles from serum. ASCs supernatant was collected and ASC-EVs were obtained using Pure Exo Exosomes Isolation Kit (101Bio, Montain View, CA, USA), following the manufacturer's protocol. The quantification of ASC-EVs protein content was determined by Bicinchoninic Protein Assay (BCA method) following the manufacturer's protocol (Thermo ScientificTM, Milan, Italy BCATM Protein Assay).

ASC-EVs size distribution and concentration were measured by Nanoparticle Tracking Analysis (NTA) using a Nanosight NS300 (Malvern Instruments, Malvern, UK). For this analysis, five video recordings with duration of 1 min were performed and analyzed for each sample. Camera level and the detection threshold were set in the acquisition and analysis, respectively, in order to achieve a concentration between 20 and 120 particles/frame. The NTA 3.4 software version was used to acquire and analyze the sample videos. The results are reported as the mean ± SEM of 3 measurements. For the morphological characterization of ASC-EVs, cryo-electron microscopy (cryo-EM) was used, (as described in[25,26]). Briefly, ASC-EVs were adsorbed onto glow-discharged holey carbon grids (QUANTIFOIL, Germany). Grids were blotted at 95% humidity and rapidly plunged into liquid ethane with the aid of VITROBOT (Maastricht Instruments BV, Maastricht, Netherlands). Vitrified samples were imaged at liquid nitrogen temperature using a JEM-2200FS/CR transmission electron microscope (JEOL, Tokyo, Japan) equipped with a field emission gun and operated at an acceleration voltage of 200 kV.

To further confirm ASC-EVs purification, the immunoblotting analysis was performed: ASC-EVs proteins were denatured, separated on 4-12% polyacrylamide gels and transferred onto a nitrocellulose membrane. Antibodies against murine CD9 (55 kDa, 1:1000; ab263019; Abcam, Cambridge, UK), HSP70 (70 kDa, 1:1000; ab181606; Abcam), ALIX (96 kDa, 1:1000; ab275377; Abcam) and GM-130 (130 kDa, 1:1000; ab52649; Abcam) were used. IgG HRP-conjugated secondary antibodies (Dako Agilent, Milan, Italy) were used to hybridize the membranes which subse-

quently were developed with a chemiluminescent HRP substrate and observed with G:BOX F3 GeneSys (Syngene, Cambridge, UK). ASCs lysates were considered a positive control.

Animals

In the study male transgenic mice overexpressing human SOD1 carrying a Gly93-Ala mutation (SOD1(G93A)) (strain designation B6SJL-TgN[SOD1-G93A]1Gur, stock number 002726) purchased from Jackson Laboratories (Bar Harbor, ME, USA) were used to avoid gender-dependent variabilities.[7] Animals were maintained in pathogen-free cages with climate-control and were housed with food and water *ad libitum* following the current European Community laws. All mouse experiments were carried out in accordance with experimental guidelines approved by the University of Verona Committee on Animal Research (CIRSAL) and by the Italian Ministry of Health (project identification code 710/2018-PR, approved 24/09/2018). Transgenic mice were discriminated from WT littermates by a polymerase chain reaction to identify the presence of the mutated human SOD1 gene (primers for SOD1 gene were forward (113) 5′-CATCAGCCCTAATC-CATCTGA-3′ and reverse (114) 5′-CGCGACTAACAAT-CAAAGTGA-3′; while for the housekeeping gene interleukin-2 receptor (IL-2R) the primers were forward (42) 5′-CTAGGC-CACAGAATTGAAAGATCT-3′; reverse (43) 5′-GTAGGTG-GAAATTCTAGCATCATCC-3′).

Motor tests

To evaluate the progression of the disease and the efficacy of ASC-EVs treatment, SOD1(G93A) mice were monitored starting from 50 days of life by motor performance examination: mice were evaluated weekly for body weight, neurological test and paw grip endurance (PaGE) test. The neurological scoring test was evaluated according to the following scale: 4, normal (no signs of motor dysfunction); 3, hind limb tremors when the mice were suspended by their tails; 2, gait irregularities; 1, dragging at least one hind limb; and 0, inability to right themselves within 30 s when placed supine. The PaGE test assessed the grip strength of the animals by placing them on an inverted metal grid. Each mouse had up to two attempts to hold onto the grid, with a maximum time of 120 s. The latency time, or the time until the hind limbs detached, was recorded.

The rotarod test evaluated motor coordination by placing the mice in a rotor tube (Acceler Rota-Rod 7650; Ugo Basile, Varese, Italy) set at a constant speed of 16 rpm. The cut-off time was 180 s, and mice that failed the test were given three attempts with a 5-min rest between each. The longest latency time was recorded.

Animals failed the PaGE or rotarod tests if they could not reach the cut-off time. Clinical onset was determined when a mouse failed the PaGE test. Humane endpoints, established and monitored according to the Ethical Committee of the University of Verona, dictated that animals with a neurological score of 0 were sacrificed, and their survival time was recorded.

ASC-EVs administration

To evaluate the therapeutic effects of ASC-EVs on SOD1(G93A) mice, a total number of 12 animals were divided randomly into ASC-EVs-treated group (ASC-EVs) and PBS-treated group (PBS) (n=7 ASC-EVs, 5 PBS). ASC-EVs were administered in SOD1(G93A) mice with i.n. injections from the onset of the clinical sign until the end-stage of the pathology, every 4 days. For each injection, the treated mice received 3 µg of ASC-EVs, while the control mice received sterile PBS. The total amount of injected solution was 10 µL for i.n. administration. In particular, the animals were placed in supine position to enhance the ASC-EVs absorption from the nasal cavity and brain's uptake and avoid

drainage into the trachea and esophagus. The administration of the total volume is gradually released with the help of a micropipette into the nostrils alternatively over a period of 20 s to allow the drop to be snorted.

Lumbar spinal cord motor neurons stereological count

At the end-stage of the disease, SOD1(G93A) mice treated with 3 µg of ASC-EVs and their control littermates (n=7 ASC-EVs, 5 PBS) were deeply anesthetized and transcardially perfused with PBS 0.1 M followed by paraformaldehyde (PFA) 4%. The spinal cords were dissected out and 2 h of post-fixation in PFA 4% was performed. The samples were soaked overnight in a 30% sucrose solution, then embedded and frozen in cryostat medium (Killik, Bio-Optica, Milan, Italy). They were serially sectioned at 15 µm using a cryostat. The sections were mounted on Surgipath® Apex™ Superior Adhesive Slides (3800080E; Leica Biosystems Italia, Milan, Italy).

For Nissl staining, the slides were air-dried and then washed in water for 30 s. The sections were stained with a 0.2% cresyl violet solution for 8 min, followed by gradual immersion in increasing concentrations of ethanol, mounted with Entelan after immersion in xylene and covered with a cover glass.

Positively stained MNs in the ventral horns (L1-L5 tract) were stereologically counted at 40x magnification (one out of every fifth 15 µm-thick section was reconstructed) using a computer-assisted microscope and StereoInvestigator software (MicroBrightField Inc., Williston, VT, USA). MNs were counted if they had a diameter of 16 µm and were located in the ventral somatic columns. The cell density was expressed as the number of MNs/mm².

Immunohistochemistry of NMJs and muscle fibers staining

ASC-EVs treated SOD1(G93A) mice and their relative controls (n=7 ASC-EVs, 5 PBS) were deeply anesthetized and transcardially perfused with 0.1 M PBS and 4% paraformaldehyde at the end stage of the disease. The hindlimb gastrocnemius muscle was dissected, post-fixed for 2 h, soaked in 30% sucrose, embedded in OCT, and longitudinally sectioned at 20 µm using a cryostat. The sections were placed on Surgipath® Apex™ Superior Adhesive Slides (3800080E; Leica Biosystems Italia).

The sections were labelled for postsynaptic acetylcholine receptors using CF543-conjugated α-bungarotoxin (αBTx, 1:500, Biotium, DBA Italia Srl, Milan, Italy) for 25 min at room temperature. Presynaptic motor terminals were stained with a primary antibody against neurofilament H (NF-H; 1:100, Chemicon, Merck, Milan, Italy) overnight at 4°C. Subsequently the sections were incubated with a species-specific Alexa Fluor 488 secondary antibody in 2% NDS in PBS (1:1000; Invitrogen, Thermo Fisher Scientific, Milan, Italy) for 1 h at room temperature, followed by DAPI (1:1000; Santa Cruz Biotechnology, DBA Italia Srl, Milan, Italy) for 15 min at room temperature. Dako Fluorescence Mounting Medium (Agilent, CA, USA) was used to mount the sections. No specific binding of the secondary antibody was used as negative control, performed with the omission of primary antibody. Wild-type mice were used as positive control for innervated NMJs.

The gastrocnemius muscle was examined for muscle fibers study by hematoxylin-eosin (HE) staining. The hindlimb muscle was transversely cut at 20 µm with cryostat and the sections were stained with hematoxylin for 40 s and with eosin for 30 s. The sections were dehydrated in ascending ethanol solution, mounted with Entelan (Merck, Darmstadt, Germany) after immersion in xylene. The sections were observed by optical microscopy (Olympus

BX63; Olympus Life Science Solutions, Center Valley, PA, USA). A total number of 100 fibers were examined for each mouse. The area of gastrocnemius fibers was measured by ImageJ software.

Statistical analysis

Motor performances were analyzed by Two-way univariate analysis of variance (ANOVA) and Bonferroni *post hoc* tests to evaluate statistical differences between the two mice groups. Data are expressed as mean ± SEM. Statistical analysis of the animals' survival was evaluated by Gehan-Breslow-Wilcoxon test. Two-tailed Student's *t*-test was performed for the stereological MNs count and the data from the skeletal muscle analysis. Data are reported as mean ± SEM. GraphPad Prism 5 Software was used for all statistical analysis. Significance was accepted at $p<0.05$.

Results

ASCs release small EVs in culture medium

EVs were isolated from ASCs supernatant and their protein concentration was quantified obtaining a yield of proteins for each isolation about 200 µg/mL. ASC-EVs were analyzed and quantified by NTA: the concentration of EVs was $4.94E10^9 ± 5.03E10^7$ particles/mL, with a particle diameter mode of 157.0 nm (Figure 1A). Morphological characteristics of EVs were performed *via*

cryo-EM to visualize ASC-EVs of different sizes and morphology. Most of the ASC-EVs have an intact single lipid bilayer/membrane with round shape (Figure 1B). Moreover, we observed double and multilayer vesicles with two or more vesicles contained inside a larger one (Figure 1C). The EVs morphological variants were in accordance with previously published observation obtained in biological fluids and cell culture media using cryo-EM.[28-30] All observed vesicles reported diameter measurements compatible with small EVs.[31] Moreover, the presence of typical markers of EVs[32] identified through CD9, HSP-70 and ALIX antibodies was assessed by western blot (Figure 1D). GM-130 was used as negative control. All the evaluated parameters confirm that size, morphology, and the presence of specific protein markers are consistent with ASC-EVs.

The intranasal administration of ASC-EVs improves the motor performance of SOD1(G93A) mice at early stage

We administered ASC-EVs i.n. a 3-fold concentration (3 µg/mL) compared to the ASC-EVs concentration previously used in Bonafede *et al*[17] starting from the clinical onset of pathology (defined in the Materials and Methods section) until the end-stage of disease (around 11 weeks) every 4 days. The mice were monitored with PaGE and Rotarod tests to determine respectively, the grip strength and the motor coordination of the treated mice. The PaGE test showed a global improvement of motor performance of
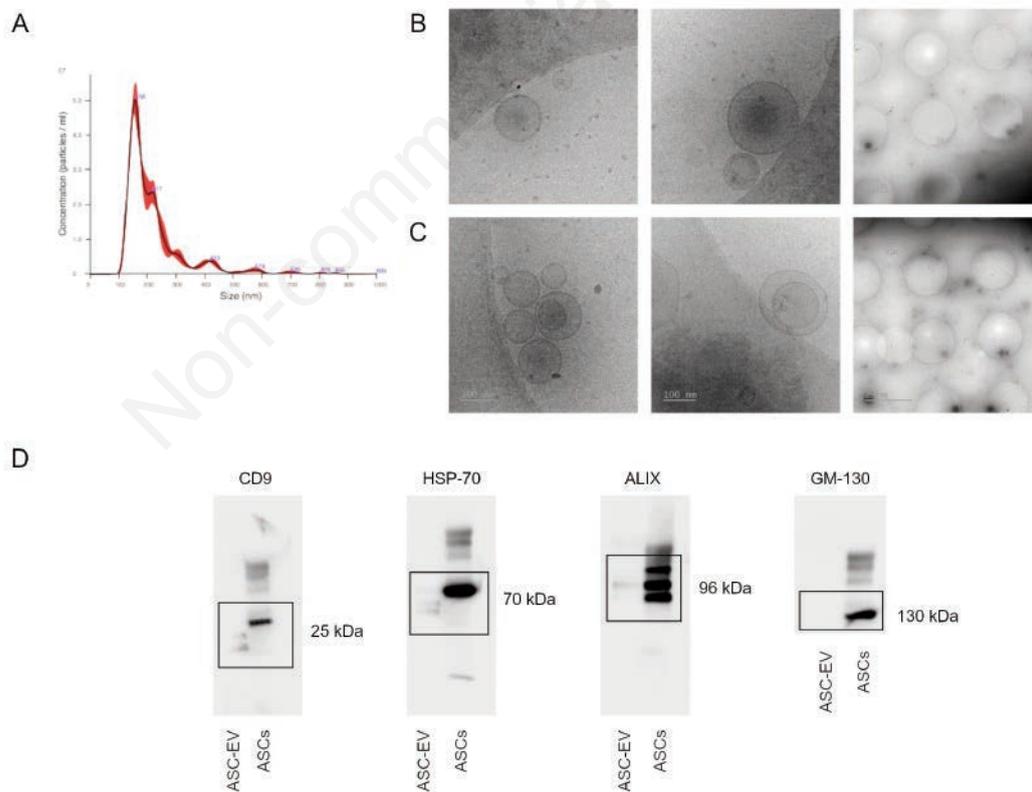
Figure 1. Characterization of ASC-EVs. **A**) NTA profile for concentration and particle size of the ASC-EVs. **B**) Representative cryo-EM images of ASC-EVs with single membrane layer. **C**) Representative cryo-EM images of ASC-EVs with multiple layers; magnification: 25kx, scale bar: 100 nm; magnification: 2000x, scale bar: 2 µm. **D**) Western blot of typical EVs markers: CD9 (25 kDa), HSP70 (70 kDa) and Alix (96 kDa) on ASC-EVs; GM-130 (130 kDa) was used to exclude the presence of Golgi's proteins. ASCs lysates (ASCs) were used as a positive control.

the ASC-EVs-treated mice as compared with the PBS control group, with significant differences already at the 1st week which persist up to 3 weeks after clinical onset (week 1 $p=0.0389$; week 2 $p=0.0008$; week 3 $p=0.0183$ respectively) maintaining constant their motor performance (Figure 2A). Concerning the Rotarod test, no significant difference was observed in ASC-EVs injected mice compared to PBS injected controls (*data not shown*). No significant effects were observed as regards to the lifespan of ASC-EVs treated mice (Figure 2B).

The intranasal administration of ASC-EVs improves the survival of Lumbar Spinal Cord MNs in SOD1(G93A) mice

Given the results obtained in PaGE test, at the late phase of the disease (where we observed a motor decline) we verify the histological modification in the lumbar spinal cord to evaluate the effect of ASC-EVs on MNs. We performed the stereological count of lumbar MNs on sections from L1-L5 metamers of the spinal cord.
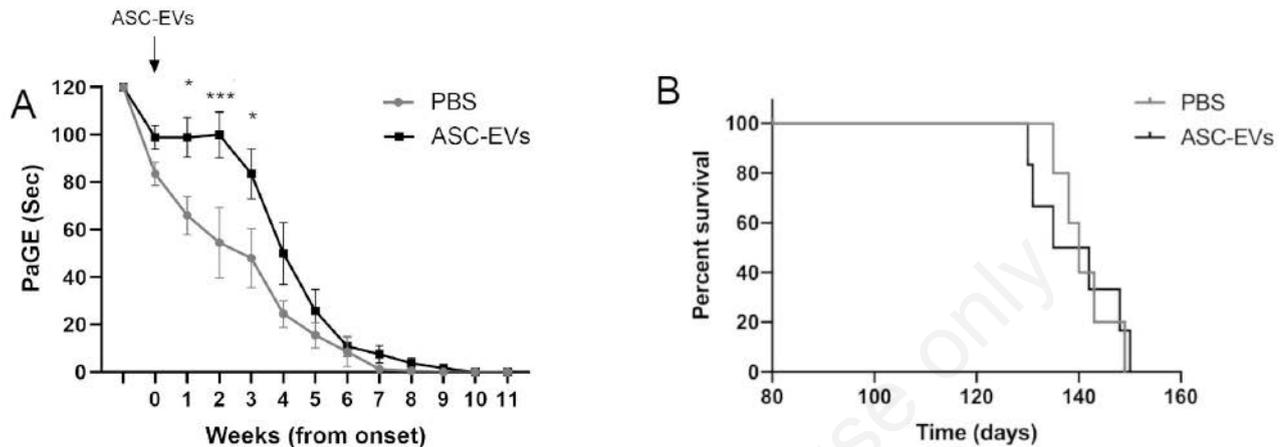
Figure 2. Motor performances and survival of SOD1(G93A) mice treated with ASC-EVs. **A**) The paw grip endurance (PaGE) test shows a global improvement of motor performance of the ASC-EVs-treated mice as compared with the PBS control group, with significant differences from 1 to 3 weeks after clinical onset; *p<0.05, ***p<0.001. **B**) The graph shows the percentage of survival of ASC-EVs-treated mice compared with the PBS control group. Data are represented as mean ± SEM.
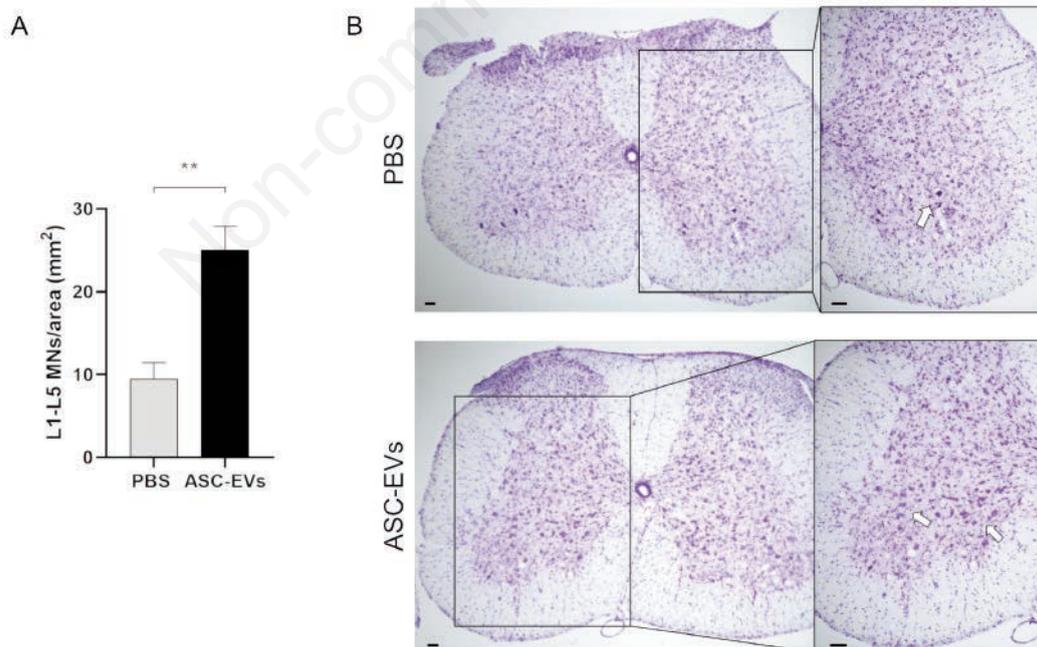
Figure 3. Neuroprotective effect of ASC-EVs treatment on lumbar MNs in SOD1(G93A) mice. **A**) The graph shows a significantly higher MN number (expressed as cell density) for the ASC-EVs injected mice compared to PBS injected controls (**p<0.005) at the end-stage of the disease. Data are represented as mean ± SEM. **B**) Representative Nissl staining of lumbar spinal cord MNs of PBS and ASC-EVs treated mice. Magnification: 4x, 10x; scale bar: 50 μm.

ASC-EVs administration produced a significant increase in surviving MNs approximately of 2.6-fold (*p*=0.0023) as compared with the PBS control mice (Figure 3 A,B).

The intranasal administration of ASC-EVs preserves the NMJs structure in SOD1(G93A) mice

The significant increase in MNs survival after the injection of ASC-EVs in SOD1(G93A) mice was correlated with NMJs observations. Indeed, a colocalization of the signal produced by presynaptic NF-H and the postsynaptic αBTx indicating a higher number of innervated NMJs in SOD1(G93A) mice treated with ASC-EVs compared to PBS-injected control mice at the end-stage (p=0.0215) (Figure 4 A,B). Surprisingly, the morphological analysis of gastrocnemius fibers did not show significant differences in ASC-EVs treated mice compared to controls (Figure 4 C,D).

Discussion

ALS is a fatal disease that currently lacks effective therapies. The approved drugs for its treatment appear to have only a moderate effect on disease progression and curative therapeutic options capable of preventing or halting disease progression are still unknown.[2,33-35]

In recent years, therapies based on the use of stem cells and their secretome are considered to be promising therapeutic approaches for ALS. Indeed, previous studies have shown the extensive neuroprotective potential in several *in vitro* and *in vivo* models of ALS through the release of extracellular vesicles derived from MSCs.[16,17,36,37] The EVs, thanks to their content of nucleic acids, proteins and lipids, appear to be an effective non-cellular therapy without producing possible side effects reported by their parental cells.[31,38]

In our previous study we administered both i.v. and i.n. small ASC-EVs (exosomes) in SOD1(G93A) mice starting from the onset of the disease. Our data showed, with both administration routes, that ASC-EVs localize in damaged brain areas of SOD1 mice and are able to produce significant improvements in motor tests, increasing the number of MNs and preserve their NMJs at the recorded time point of animal's best motor performance.[17] Although we showed several improvements following the treatment, unfortunately there were no visible changes in the survival of the animals. Indeed, establishing the correct "therapeutic regimen" for the use of ASC-EVs could influence the therapeutic outcomes. The definition of the correct "therapeutic regimen" includes the evaluation of the optimal dosage, the route of administration and the frequency of treatments.[39, 40]

In our previous study we have already identified the i.n. route as an excellent alternative to other routes of administration capable of producing effects comparable to systemic administration but in a much less invasive manner and with the possibility of being more usable from a translational point of view.[17] Regarding the ASC-EVs dosage, the rationale for EV dose selection and treatment frequency is largely variable[41] and dose-response studies are difficult to correlate given the enormous variables. Although MSC-EVs are generally considered relatively safe and poorly toxic,[42] an overall understanding of their toxicity has not been fully elucidated and some toxic effects were reported.[16] In this current work we injected
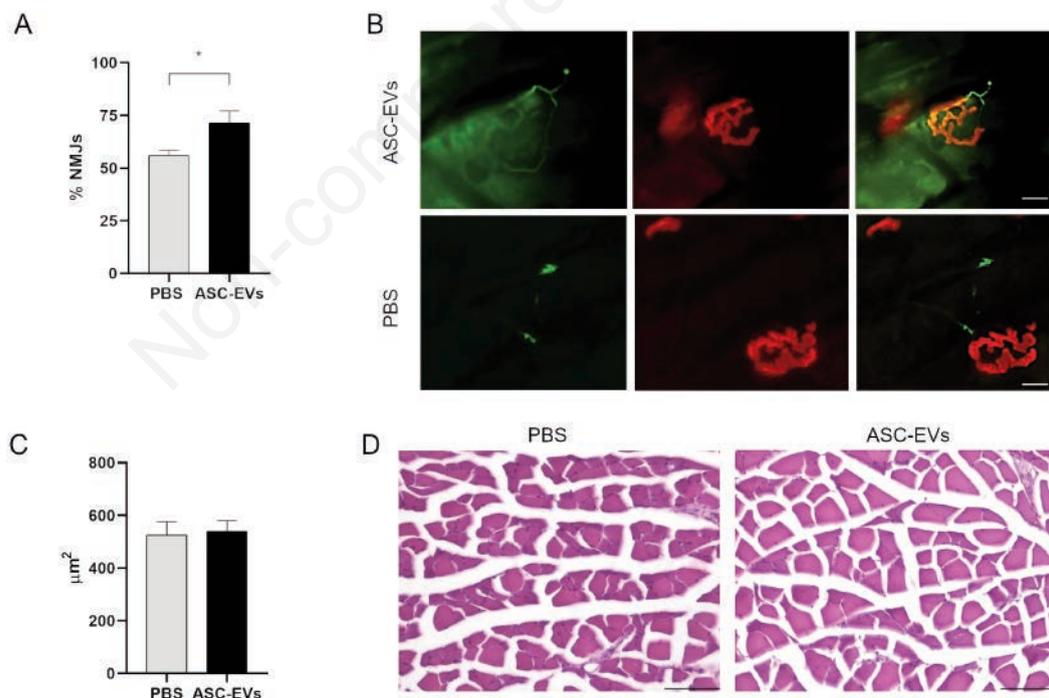
Figure 4. ASC-EVs effects on NMJs and muscle fibers. **A**) The graph shows a significant increase in colocalization of NF-H and αBTx in SOD1(G93A) mice injected with ASC-EVs as compared with PBS-injected control mice (*p<0.05). Data are represented as mean ± SEM. **B**) Representative images of the NMJ architecture: on the upper panel the colocalization of presynaptic NF-H (green) and αBTx (red); on the lower panel the degeneration of the NMJ; magnification: 40x, scale bar: 25 µm. **C**) The graph shows the quantitative analysis of the average muscular fiber area in ASC-EVs injected SOD1(G93A) mice and PBS control mice; data are shown as mean ± SEM. **D**) Representative images of HE staining in SOD1(G93A) mice treated with PBS or ASC-EVs. Magnification: 20x; scale bar: 100 µm.

i.n. a 3-fold concentration of ASC-EVs (compared to our previous study) in SOD1(G93A) mice in order to improve the clinical and neuropathological outcomes of affected mice. This dose of ASC-EVs appears to be the most suitable concentration to obtain major improvements compared to the previous experimentation without the risk of overdose or side effects.

Following the injections of ASC-EVs in SOD1(G93A) transgenic mice, we observed a significant improvement of their motor performance already at the first week after the first injection which persist up to 3 weeks after clinical onset, suggesting a beneficial clinical effect in the early stage of the disease which is lost with the disease progression. The ineffectiveness of ASC-EVs treatment in the progressive stages of the disease correlates with a failure to increase the survival of affected mice, consequently due, probably, to the SOD1 mutation which leads animals to a programmed death, and as a result, extremely difficult to counteract with ASC-EVs treatment.

Interestingly, ASC-EVs treatment showed a significant improvement in the survival of lumbar MNs, indicating that treatment with ASC-EVs is able to protect lumbar MNs from the degeneration during the progression of the disease until the end-stage. Indeed, the number of MNs observed was 2.6 times higher than in controls and approximately 50% higher than that obtained with one third of the dose, suggesting a dose-dependent increase in MN rescue. The neuroprotective effect of ASC-EVs on MNs seems to be due to the modulation of proteins involved in apoptotic processes. Indeed, we have previously demonstrated that ASC-EVs reduce proapoptotic agents such as cleaved-caspase 3 and Bax and simultaneously upregulate antiapoptotic proteins, like BCL-2α.[15] Moreover, beneficial effects of MSC-EVs on neurite growth and morphology were observed in SOD1(G93A) primary MNs due to the presence of several antioxidant and anti-inflammatory genes in MSC-EVs revealed in gene expression profile.[43] ASC-EVs treatment not only protects MNs but, concomitantly, preserves their function as indicated by a significantly higher number of innervated NMJs. It is known that NMJs become denervated during disease progression and that axon retraction bulbs are the end point of this process.[44,45] The effect of ASC-EVs on MNs protection reflects also on the maintenance of NMJs, suggesting a slowing down axon retraction. Consequently, at the end-stage of the disease the NMJ appears to be structurally intact. However, the diameter of the muscle fibers of ASC-EVs treated mice, compared to PBS injected controls, did not appear to be different. Our data indicates that i.n. ASC-EVs administration is able to rescue MNs and their axons but not impact on skeletal muscle.

Skeletal muscle involvement in ALS is generally considered as the secondary consequence of MNs degeneration. The muscle pathophysiology in ALS is controversial.[46-48] However, growing evidence sustain the hypothesis that the degenerative processes involved MNs and skeletal muscles *via* autonomous mechanisms and their cross-talk mutually influence the degeneration. This circuit creates a detrimental loop which contributes to the pathogenesis of ALS.

These considerations lead us to identify multiple therapeutic targets both at central and peripheral level. The "multi-target" approach perfectly fit with the multifactorial nature of ALS disease in which many different pathogenetic mechanisms and several affected districts are described.[49-51]

Some authors described experimental paradigms to mitigate the global degeneration at both central and peripheral levels simultaneously. Stem cells and their secretome were injected *via* intraspinal or intrathecal and contemporary at peripheral level, intramuscular,[52,53] demonstrating beneficial effects.

Overall, our study identified the i.n. administration of ASC-EVs as a potential early treatment to counteract the central neurodegeneration in SOD1(G93A) mice, acting principally on MNs.

This strategy could pave the way for new experimental therapeutic approaches which exploit a combined action of ASC-EVs directly to the central nervous system and, simultaneously, in distal sites to ameliorate the symptomatology and progression of the disease.

Acknowledgments

References

1. Hardiman O, Al-Chalabi A, Chio A, Corr EM, Logroscino G, Robberecht W, et al. Amyotrophic lateral sclerosis. Nat Rev Dis Primers 2017;3:17085.
2. Tzeplaeff L, Wilfling S, Requardt MV, Herdick M. Current state and future directions in the therapy of ALS. Cells 2023;12:1523.
3. Rosen DR, Siddique T, Patterson D, Figlewicz DA, Sapp P, Hentati A, et al. Mutations in Cu/Zn superoxide dismutase gene are associated with familial amyotrophic lateral sclerosis. Nature 1993;362:59-62.
4. Zou ZY, Zhou ZR, Che CH, Liu CY, He RL, Huang HP. Genetic epidemiology of amyotrophic lateral sclerosis: a systematic review and meta-analysis. J Neurol Neurosurg Psychiatry 2017;88:540-9.
5. Ciuro M, Sangiorgio M, Leanza G, Gulino R. A Meta-analysis study of SOD1-mutant mouse models of ALS to analyse the determinants of disease onset and progression. Int J Mol Sc. 2022;24:216.
6. Gurney ME, Pu H, Chiu AY, Dal Canto MC, Polchow CY, Alexander DD, et al. Motor neuron degeneration in mice that express a human Cu,Zn superoxide dismutase mutation. Science 1994;264:1772-5.
7. Aishwarya R, Abdullah CS, Remex NS, Nitu S, Hartman B, King J, et al. Pathological sequelae associated with skeletal muscle atrophy and histopathology in G93A*SOD1 mice. Muscles 2023;2:51-74.
8. Maragakis NJ, Rothstein JD. Mechanisms of disease: astrocytes in neurodegenerative disease. Nat Clin Pract Neurol 2006; 2:679-89.
9. Perrin S. Preclinical research: make mouse studies work. Nature 2014;507:423-5.
10. Philips T, Rothstein JD. Rodent models of amyotrophic lateral sclerosis. Curr Protoc Pharmacol 2015;69:5.67.1-5.67.21.
11. Gugliandolo A, Bramanti P, Mazzon E. Mesenchymal stem cells: a potential therapeutic approach for amyotrophic lateral sclerosis? Stem Cells Int 2019;2019:3675627.
12. Marconi S, Bonaconsa M, Scambi I, Squintani GM, Rui W, Turano E, et al. Systemic treatment with adipose-derived mesenchymal stem cells ameliorates clinical and pathological features in the amyotrophic lateral sclerosis murine model. Neuroscience 2013;248:333-43.
13. Shalaby SM, Sabbah NA, Saber T, Abdel Hamid RA. Adipose-derived mesenchymal stem cells modulate the immune response in chronic experimental autoimmune encephalomyelitis

model. IUBMB Life 2016;68:106-15.

14. Gu Z, Akiyama K, Ma X, Zhang H, Feng X, Yao G, et al. Transplantation of umbilical cord mesenchymal stem cells alleviates lupus nephritis in MRL/lpr mice. Lupus 2010;19:1502-14.

15. Bonafede R, Brandi J, Manfredi M, Scambi I, Schiaffino L, Merigo F, et al. The anti-apoptotic effect of ASC-exosomes in an in vitro ALS model and their proteomic analysis. Cells 2019;8:1087.

16. Bonafede R, Scambi I, Peroni D, Potrich V, Boschi F, Benati D, et al. Exosome derived from murine adipose-derived stromal cells: neuroprotective effect on in vitro model of amyotrophic lateral sclerosis. Exp Cell Res 2016;340:150-8.

17. Bonafede R, Turano E, Scambi I, Busato A, Bontempi P, Virla F, et al. ASC-exosomes ameliorate the disease progression in SOD1(G93A) murine model underlining their potential therapeutic use in human ALS. Int J Mol Sci 2020;21:3651.

18. Giunti D, Marini C, Parodi B, Usai C, Milanese M, Bonanno G, et al. Role of miRNAs shuttled by mesenchymal stem cell-derived small extracellular vesicles in modulating neuroinflammation. Sci Rep 2021;11:1740.

19. Provenzano F, Nyberg S, Giunti D, Torazza C, Parodi B, Bonifacino T, et al. Micro-RNAs shuttled by extracellular vesicles secreted from mesenchymal stem cells dampen astrocyte pathological activation and support neuroprotection in in-vitro models of ALS. Cells 2022;11:3923.

20. Gnecchi M, Danieli P, Malpasso G, Ciuffreda MC. Paracrine mechanisms of mesenchymal stem cells in tissue repair. Methods Mol Biol 2016;1416:123-46.

21. Melling GE, Carollo E, Conlon R, Simpson JC, Carter DRF. The Challenges and possibilities of extracellular vesicles as therapeutic vehicles. Eur J Pharm Biopharm 2019;144:50-6.

22. Witwer KW, Théry C. Extracellular vesicles or exosomes? On primacy, precision, and popularity influencing a choice of nomenclature. J Extracell Vesicles 2019;8:1648167.

23. Peroni D, Scambi I, Pasini A, Lisi V, Bifari F, Krampera M, et al. Stem molecular signature of adipose-derived stromal cells. Exp Cell Res 2008;314:603-15.

24. Constantin G, Marconi S, Rossi B, Angiari S, Calderan L, Anghileri E, et al. Adipose-derived mesenchymal stem cells ameliorate chronic experimental autoimmune encephalomyelitis. Stem Cells 2009;27:2624-35.

25. Pascua-Maestro R, Gonzalez E, Lillo C, Ganfornina MD, Falcon-Perez JM, Sanchez D. Extracellular vesicles secreted by astroglial cells transport apolipoprotein D to neurons and mediate neuronal survival upon oxidative stress. Front Cell Neurosci 2018;12:526.

26. Royo F, Moreno L, Mleczko J, Palomo L, Gonzalez E, Cabrera D, et al. Hepatocyte-secreted extracellular vesicles modify blood metabolome and endothelial function by an arginase-dependent mechanism. Sci Rep 2017;7:42798.

27. Bankole O, Scambi I, Parrella E, Muccilli M, Bonafede R, Turano E, et al. Beneficial and sexually dimorphic response to combined HDAC inhibitor valproate and AMPK/SIRT1 Pathway activator resveratrol in the treatment of ALS mice. Int J Mol Sci 2022;23:1047.

28. Zabeo D, Cvjetkovic A, Lasser C, Schorb M, Lotvall J, Hoog JL. Exosomes purified from a single cell type have diverse morphology. J Extracell Vesicles 2017;6:1329476.

29. Emelyanov A, Shtam T, Kamyshinsky R, Garaeva L, Verlov N, Miliukhina I, et al. Cryo-electron microscopy of extracellular vesicles from cerebrospinal fluid. PLoS One 2020;15:e0227949.

30. Las Heras K, Royo F, Garcia-Vallicrosa C, Igartua M, Santos-Vizcaino E, Falcon-Perez JM, et al. Extracellular vesicles from hair follicle-derived mesenchymal stromal cells: isolation, characterization and therapeutic potential for chronic wound healing. Stem Cell Res Ther 2022;13:147.

31. Doyle LM, Wang MZ. Overview of extracellular vesicles, their origin, composition, purpose, and methods for exosome isolation and analysis. Cells 2019;8:727.

32. Kowal J, Arras G, Colombo M, Jouve M, Morath JP, Primdal-Bengtson B, et al. Proteomic comparison defines novel markers to characterize heterogeneous populations of extracellular vesicle subtypes. Proc Natl Acad Sci USA 2016;113:E968-77.

33. Fang T, Al Khleifat A, Meurgey JH, Jones A, Leigh PN, Bensimon G, et al. Stage at which riluzole treatment prolongs survival in patients with amyotrophic lateral sclerosis: a retrospective analysis of data from a dose-ranging study. Lancet Neurol 2018;17:416-22.

34. Staff NP, Jones DT, Singer W. Mesenchymal stromal cell therapies for neurodegenerative diseases. Mayo Clin Proc 2019;94:892-905.

35. Swindell WR, Kruse CPS, List EO, Berryman DE, Kopchick JJ. ALS blood expression profiling identifies new biomarkers, patient subgroups, and evidence for neutrophilia and hypoxia. J Transl Med 2019;17:170.

36. Garbuzova-Davis S, Borlongan CV. Stem cell-derived extracellular vesicles as potential mechanism for repair of microvascular damage within and outside of the central nervous system in amyotrophic lateral sclerosis: perspective schema. Neural Regen Res. 2021;16:680-1.

37. Lee M, Ban JJ, Kim KY, Jeon GS, Im W, Sung JJ, et al. Adipose-derived stem cell exosomes alleviate pathology of amyotrophic lateral sclerosis in vitro. Biochem Biophys Res Commun 2016;479:434-9.

38. Zeng ZL, Xie H. Mesenchymal stem cell-derived extracellular vesicles: a possible therapeutic strategy for orthopaedic diseases: a narrative review. Biomater Transl 2022;3:175-87.

39. Ciervo Y, Ning K, Jun X, Shaw PJ, Mead RJ. Advances, challenges and future directions for stem cell therapy in amyotrophic lateral sclerosis. Mol Neurodegener 2017;12:85.

40. Jin J, Sklar GE, Min Sen Oh V, Chuen Li S. Factors affecting therapeutic compliance: A review from the patient's perspective. Ther Clin Risk Manag 2008;4:269-86.

41. Gupta D, Zickler AM, El Andaloussi S. Dosing extracellular vesicles. Adv Drug Deliv Rev 2021;178:113961.

42. Cheng X, Zhang G, Zhang L, Hu Y, Zhang K, Sun X, et al. Mesenchymal stem cells deliver exogenous miR-21 via exosomes to inhibit nucleus pulposus cell apoptosis and reduce intervertebral disc degeneration. J Cell Mol Med 2018;22:261-76.

43. Gschwendtberger T, Thau-Habermann N, von der Ohe J, Luo T, Hass R, Petri S. Protective effects of EVs/exosomes derived from permanently growing human MSC on primary murine ALS motor neurons. Neurosci Lett 2023;816:137493.

44. Alhindi A, Boehm I, Chaytow H. Small junction, big problems: Neuromuscular junction pathology in mouse models of amyotrophic lateral sclerosis (ALS). J Anat 2022;241:1089-107.

45. Schaefer AM, Sanes JR, Lichtman JW. A compensatory subpopulation of motor neurons in a mouse model of amyotrophic lateral sclerosis. J Comp Neurol 2005;490:209-19.

46. Dupuis L, Loeffler JP. Neuromuscular junction destruction during amyotrophic lateral sclerosis: insights from transgenic models. Curr Opin Pharmacol 2009;9:341-6.

47. Shefner JM, Musaro A, Ngo ST, Lunetta C, Steyn FJ, Robitaille R, et al. Skeletal muscle in amyotrophic lateral sclerosis. Brain 2023;146:4425-36.

48. Dadon-Nachum M, Melamed E, Offen D. The "dying-back"

phenomenon of motor neurons in ALS. J Mol Neurosci 2011;43:470-7.

49. Eisen A, Vucic S, Mitsumoto H. History of ALS and the competing theories on pathogenesis: IFCN handbook chapter. Clin Neurophysiol Pract 2024;9:1-12.

50. Bottero V, Santiago JA, Quinn JP, Potashkin JA. Key disease mechanisms linked to amyotrophic lateral sclerosis in spinal cord motor neurons. Front Mol Neurosci 2022;15:825031.

51. Maranzano A, Verde F, Colombo E, Poletti B, Doretti A, Bonetti R, et al. Regional spreading pattern is associated with clinical phenotype in amyotrophic lateral sclerosis. Brain 2023;146:4105-16.

52. Martínez-Muriana A, Pastor D, Mancuso R, Rando A, Osta R, Martínez S, et al. Combined intramuscular and intraspinal transplant of bone marrow cells improves neuromuscular function in the SOD1(G93A) mice. Stem Cell Res Ther 2020;11:53.

53. Řehořová M, Vargová I, Forostyak S, Vacková I, Turnovcová K, Kupcová Skalníková H, et al. A combination of intrathecal and intramuscular application of human mesenchymal stem cells partly reduces the activation of necroptosis in the spinal cord of SOD1(G93A) rats. Stem Cells Transl Med 2019;8:535-47.